

Fissile nuclear material identification in shielding conditions using a neutron resonance analysis technique

Fabiana Rossi ^a, Jaehong Lee ^a, Yuki Yoshimi ^b, Kota Hironaka ^a, Mitsuo Koizumi ^a, Tomooki Shiba ^a, Kazushi Terada ^c, Jun-ichi Hori ^c

^a Japan Atomic Energy Agency, Integrated Support Center for Nuclear Non-proliferation, Security and Human Resource Development, 2-4 Shirane, Tokai-mura, Ibaraki, Japan, 319-1195

^b OUTSOURCING TECHNOLOGY Inc., Marunouchi Trust Tower Main 16 & 17F, 1-8-3 Marunouchi, Chiyoda-ku, Tokyo 100-0005, Japan

^c Kyoto University, Institute for Integrated Radiation and Nuclear Science, 2-1010 Asashiro-Nishi, Kumatori-cho, Osaka 590-0494

Abstract:

The Japan Atomic Energy Agency's Integrated Support Center for Nuclear Non-proliferation, Security and Human Resource Development is developing an advanced neutron resonance analysis system for the identification and quantification of fissile materials. This system integrates three complementary techniques: neutron resonance transmission analysis, neutron resonance capture analysis, and neutron resonance fission neutron analysis. High-energy neutrons generated using the electron linear accelerator beamline at the Institute for Integrated Radiation and Nuclear Science of Kyoto University, are moderated and directed through a series of collimators to the experimental area, where the sample is positioned. Surrounding the sample, plastic scintillators with neutron-gamma pulse shape discrimination capabilities allow for the collection and analysis of prompt gamma rays and fission neutron signals, while un-scattered neutrons passing through the sample are detected by a downstream glass scintillator. We conducted a series of experiments using natural uranium samples with different thicknesses enclosed in lead shielding. The results show that even if the presence of lead generates significant background noise due to neutron scattering and reflection, a clear identification of ²³⁵U signatures is possible. These findings highlight the system's versatility and effectiveness in shielding scenarios, offering a promising tool for nuclear security and non-proliferation applications.

Keywords:

neutron resonance, natural uranium, mass correlation, safeguards, non-proliferation

1. Introduction

Over the last decade, the Japan Atomic Energy Agency (JAEA) and its Integrated Support Center for Nuclear Non-proliferation, Security and Human Resource Development (ISCN) have

been developing advanced active non-destructive assay (NDA) technologies to improve nuclear material detection and verification for safeguards and security applications. This project, funded by the Ministry of Education, Culture, Sports, Science and Technology (MEXT), aims to supplement current safeguards verification methods, particularly for highly radioactive nuclear materials where passive NDA techniques are ineffective due to high neutron and gamma-ray backgrounds. Key applications include the analysis of materials from reprocessing plants, spent fuel, fuel debris, and new fuel materials for advanced reactors.

Among the various active NDA technologies under development, Neutron Resonance Analysis (NRA) has emerged as a particularly promising method for identifying and quantifying nuclear materials. Traditionally, NRA combines Neutron Resonance Transmission Analysis (NRTA) [1, 2, 3, 4, 5] and Neutron Resonance Capture Analysis (NRCA) [3, 6]; however, we are integrating these techniques with Neutron Resonance Fission Neutron Analysis (NRFNA) [7, 8]. This comprehensive approach enhances sensitivity and enables simultaneous detection, significantly improving the identification and quantification of fissile materials. Previous experiments conducted at the Institute for Integrated Radiation and Nuclear Science at Kyoto University using natural and enriched uranium samples demonstrated the system's effectiveness in detecting small amounts of fissile nuclear material under unshielded conditions. These results established the foundation for further exploration of NRA capabilities in more complex environments.

Building on these previous experiences, our current study extends the application of NRA techniques to shielded nuclear materials. This paper presents our experimental efforts using natural uranium samples embedded in thick lead shielding, details the advanced pulse shape discrimination (PSD) analysis methods, and demonstrates successful mass correlation using

neutron signals from NRFNA, specifically from fission neutron detection in the plastic scintillators. While NRCA gamma-ray signals were also investigated, further analysis is required for reliable mass correlation. Our results highlight the system’s ability to identify fissile material signatures despite substantial shielding, reinforcing its potential as a valuable tool for both nuclear safeguards and security applications.

2. Experimental setup

Experiments were conducted at Kyoto University, Institute for Integrated Radiation and Nuclear Science, using the KURNS-LINAC [9, 10]. The LINAC parameters were set as in previous experiments [7, 11], with a repetition rate of 50 Hz and a pulse width of 2 μ s. The moderated neutron beam, which has a diameter of 5 cm, reaches the measurement room approximately 12.6 meters from the source. The beam was further collimated using borated polyethylene bricks, for a total dimension of 40×30×20 cm³, and lead bricks of the same final dimensions, each with a 3 cm square hole in the center.

In contrast to the previous experiment, with quadrangular prism EJ-299M scintillators [7], new scintillators were used to improve neutron/gamma pulse-shape discrimination. Specifically, six hexagonal EJ-276D scintillators [12], each with a side length of 6.4 cm and a thickness of 10 cm, were employed. These scintillators were coupled with Hamamatsu H6527 photomultiplier tubes [13]. The experimental setup is shown in Figure 1. Three detectors were symmetrically positioned on each side of the sample. A 2.0 cm thick lead shield was placed between the sample and the detectors, and additional shielding (up to 15 cm thick) was added on the side facing the beam direction. This shielding reduced both the room background from the 2.2 MeV gamma rays produced by neutron capture on hydrogen during thermalization of the neutron beam with the water moderator and the gamma rays emitted by the sample. Downstream from the beam-to-sample line, a 1-cm thick ⁶Li-glass scintillator (GS20) was placed, as shown in Figure 1. This scintillator is used to collect transmitted neutrons and is employed in Neutron Resonance Transmission Analysis (NRTA) measurements.

As in the previous experiment [7], natural uranium samples were used. The samples were wrapped in aluminum foil to achieve thicknesses of 0.15, 0.30, and 0.60 cm. For this experiment, the samples were placed inside a lead box with a 2.0 cm thickness, as shown in Figure 2. This represents our first attempt to measure uranium samples within a shielding container, aiming to explore the limitations and potential of this

methodology. A summary of the different measurements performed is presented in Table 1.

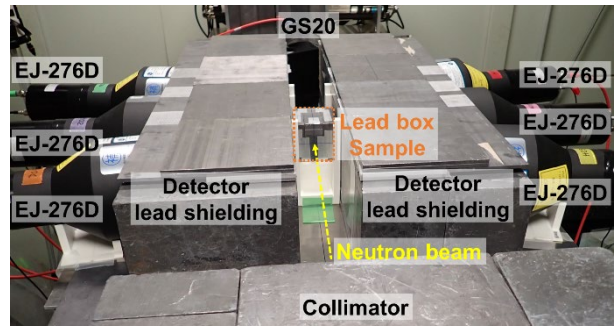


Figure 1. Experimental setup: a 3x3 cm collimator, six EJ-276D PSD detectors surrounded by lead shielding, and one GS20 detector placed downstream the beam. The sample is located within a 2cm-thick lead box in the center of the system.

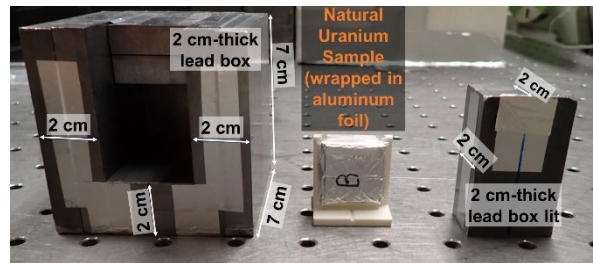


Figure 2. Details of the 2 cm-thick sample lead box and the natural uranium sample after being wrapped in aluminum foil.

Table 1. List of experimental measurements taken.

Run Number	Natural Uranium Thickness [cm]	Lead box
1831	0.60	YES
1822	0.30	YES
1845	0.15	YES
1832	NO	YES
1823	NO	NO

3. Data analysis

3.1. Acquisition Setup

The detector signals were digitized using a CAEN V1730D 16-channel digitizer operated at a sampling rate of 500 MS/s and 14-bit resolution [14]. The acquisition digitizer parameters were set to have a pre-trigger of 96 ns, used in the baseline subtraction, and a baseline threshold of 3 LSB to define pulse start times. Also, the integration gates were set to 40 ns for the short gate, and 600 ns for the long gate. For the acquisition, the pile-up rejection option was disabled to preserve statistics. Data were collected in list-mode to record each event’s short-gate charge (Q_s), long-gate charge (Q_L), and incident neutron timestamp (t_{TOF}). The readout acquisition software was executed in

binary mode, producing a log and an event file for each run.

These settings ensured that both prompt γ -ray and fission neutron pulses were fully sampled within the acquisition window. All the events raw data were then extracted from the binary files using an in-house converter and imported into the ROOT data-analysis platform [15, 16] for post-processing.

3.2. Gating

In ROOT, each detector's data were stored in a TTree. To distinguish between gamma and neutron signals, the Neutron/Gamma (n/g) pulse shape discrimination (PSD) method is used [17]. The PSD value is calculated as:

$$PSD = \frac{Q_L - Q_S}{Q_L} \quad (1)$$

where Q_S (short gate) represents the charge integrated during the early part of the pulse, and Q_L (long gate) represents the total charge integrated over the entire signal duration.

A polynomial curve is used for n/g gating to separate the neutron signal from the gamma-ray signal. Compared to conventional n/g separation, where a straight-line boundary is decided by the user using the PSD curve, this method reduces the bias introduced by user experience. Specifically, 2D histograms of Q_L and PSD were created for each detector in the range of $100 \leq Q_L \leq 10000$. An example for the 0.60 cm-thick natural uranium sample inside the lead box is shown in Figure 3. The range of Q_L is divided into 20 intervals, and the PSD projection is obtained for each interval. Neutron and gamma-ray signals are then fitted using a Gaussian fit for each Q_L interval [18]. Examples of the PSD projection for the first three Q_L intervals of the 0.60 cm-thick natural uranium sample inside the lead box are shown in Figure 4. From the fit results, the centroid of the gamma-ray Gaussian (x_0) and its standard deviation (σ) are determined. Using the standard deviation method with $x_0 \pm n\sigma$, the tail of the Gaussian is evaluated for $n = 2, 3, 4$. These points are plotted in the Q_L -PSD histogram and fitted with a sixth-degree polynomial curve within the calibration range $100 \leq Q_L \leq 10000$. For $Q_L > 10000$, the PSD separation value was kept constant at its value at $Q_L = 10000$ (the polynomial fit was not extrapolated beyond the calibrated range). The obtained separation for the 0.60 cm-thick natural uranium sample inside the lead box is shown in Figure 3.

In this study, the gamma-ray signals are considered as all the data below the 2σ polynomial curve, while neutrons are considered as the data above the 4σ curve but below a fixed PSD threshold of 0.5. This threshold was determined from the average tail of the neutron Gaussians across all Q_L intervals and rounded for consistency. Events appearing above 0.5 correspond mainly to pulse pile-up and other non-physical signals and were excluded from the analysis. Since there were no changes in the geometry or detector setup across different measurements, the run with the 0.60 cm-thick natural uranium sample inside the lead box was used as a reference for gating all other samples.

3.3. Dead-Time Correction

Dead-time correction factors were applied considering stable LINAC beam intensity, using:

$$N_c(I) = \frac{N_o(I)}{1 - \frac{\sum N_o(j)}{N_b} \frac{N_o(I)}{N_b}} \quad (2)$$

where $N_o(I)$ is the observed counts, $\sum(N_o(j))$ is the lost counts, and N_b is the number of LINAC bursts during the acquisition with a 50 Hz repetition rate [19, 20]. Lost counts due to dead-time were verified by examining the time intervals for each hexagonal detector. The number of bursts corresponds to the total events recorded in the channel dedicated to the LINAC.

3.4. Time-Of-Flight Spectra

After corrections and gating, time-of-flight (TOF) spectra were generated for both fission and transmitted neutrons and capture γ -rays from the recorded incident neutron timestamp (t_{TOF}) in μs :

$$t_{TOF} = t_0 - t_d \dots \quad (3)$$

where TOF start, t_0 , is derived from the LINAC trigger signal, which is produced when the electron beam enters the Ta-target; TOF stop, t_d , is recorded when a signal is produced in the detector. The energy of the neutron in eV can then be derived using the formula:

$$E_n = \frac{1}{2} m \left(\frac{L}{t_{TOF}} \right)^2 \quad (4)$$

where $m = 1.675 \times 10^{-27} \text{ kg}$ is the neutron mass, L in *meter* is the distance between the neutron source and the neutron detector. With a neutron beam burst of 50 Hz (corresponding to 20000 μs) and a flight path of 12.6 meter, the incident neutron energy is about 0.002 eV. Therefore, the neutron resonances of the uranium sample can

be evaluated above the energy range 0.002 eV. For γ -rays, TOF histograms were obtained from the same timestamps as for neutrons, with events classified as γ -rays by PSD binned relative to the LINAC pulse. This ensures consistent treatment of both species, analogous to the neutron TOF approach described in [11]. In the present study, the signals from the six PSD detectors are summed together to increase the overall signal. The spectra are then scaled by the measurement time and normalized to 1 hour for easy comparison. As a result, spectra like those presented in Figure 5 for the 0.60 cm sample are obtained for each run.

4. Results and discussion

The one-hour TOF gamma capture spectra obtained from the six PSD scintillators, after gating and dead-time correction, are shown in Figure 6 for all measurements listed in Table 1. The gamma-ray resonances at 6.67 eV, 20.87 eV, 36.68 eV, and 66.0 eV from the $^{238}\text{U}(n,\gamma)$ reaction are labelled and clearly visible above the background in the runs when the uranium sample was used. Since the sample is natural uranium with only 0.7% ^{235}U , the resonances from ^{238}U dominate the gamma-gated spectra due to its higher neutron capture cross-section and larger isotopic abundance. Additionally, the background between the two runs with (1832) and without (1823) the lead box increases considerably. This can be explained by the increase of scattering of gamma rays after they interact with the lead box positioned near the sample.

The one-hour TOF neutron spectra obtained from the same six PSD scintillators, after gating and dead-time correction, are shown in Figure 7. All major neutron resonances of ^{235}U , as listed in Table 2, are labeled and clearly visible for all samples. This indicates the potential for identifying fissile nuclides, such as ^{235}U , within a shielding container, using NRFNA data. One of the advantages of the neutron signal is the low background in the region of interest. Additionally, the resonance peaks from fissile nuclides, such as ^{235}U , can be enhanced.

Both gamma-ray and neutron spectra provide useful information, but they offer different advantages and challenges in the analysis of fissile materials. While capture gamma-ray resonances from ^{238}U were clearly visible, neutron spectra provided clearer identification of ^{235}U resonances, even in complex or shielded samples. The low background in the neutron spectra allows for clearer identification of fissile nuclides, while the gamma-ray spectra are more influenced by scattering and background from

surrounding materials. These differences highlight the complementary nature of gamma-ray and neutron measurements in NRA.

To quantify the fissile nuclides in the shielded sample, we performed an initial attempt to verify the linearity of resonances peak counts with the sample mass. For this analysis, we used the integrated counts from the peaks listed in Table 2, excluding the first two due to poor statistics. The run with only the lead box (1832), which served as the baseline, was used to calculate integrated counts within the same energy ranges for each peak. The results, shown in Figure 8, were analyzed for varying sample thicknesses. Each set of data points (representing the integrated counts of each resonance energy) was fitted with a first-degree polynomial. The fit quality was assessed using the reduced chi-squared statistic, χ_{red}^2 , defined as:

$$\chi_{red}^2 = \frac{\chi^2}{NDF} \quad (5)$$

where χ^2 is the chi-squared value and NDF is the number of degrees of freedom. The results show a linear correlation between the neutron peak counts and the sample mass for each of the ^{235}U peaks, with $\chi_{red}^2 \approx 1$. Although more samples are needed to evaluate the effect of sample self-shielding and to validate this methodology, NRFNA shows the potential for fissile nuclide quantification in shielded materials.

Similarly, we attempted to correlate gamma-ray peak counts with sample mass, as shown in Figure 9. Although there was an increase in the integrated number of counts with sample mass, the limited number of data points only appears to follow a quadratic trend. The apparent deviation from linearity is attributed to experimental factors such as fluctuations in generator intensity and self-shielding effects within the samples [21]. The absence of neutron monitor data prevented normalization to the source intensity; however, LINAC current monitoring indicated no significant short-term variations within individual runs, but a gradual decrease in beam intensity over the full experimental week. To better assess these effects, a dedicated neutron monitor has now been incorporated into the upgraded setup. In addition, a detailed Monte Carlo model of the experimental geometry is being developed to quantify self-shielding and improve the consistency of the results across different sample configurations. As a result, these results will not be discussed further in this paper. Further experiments will be planned in the future NRA system to more accurately assess the behavior of gamma rays in these measurements.

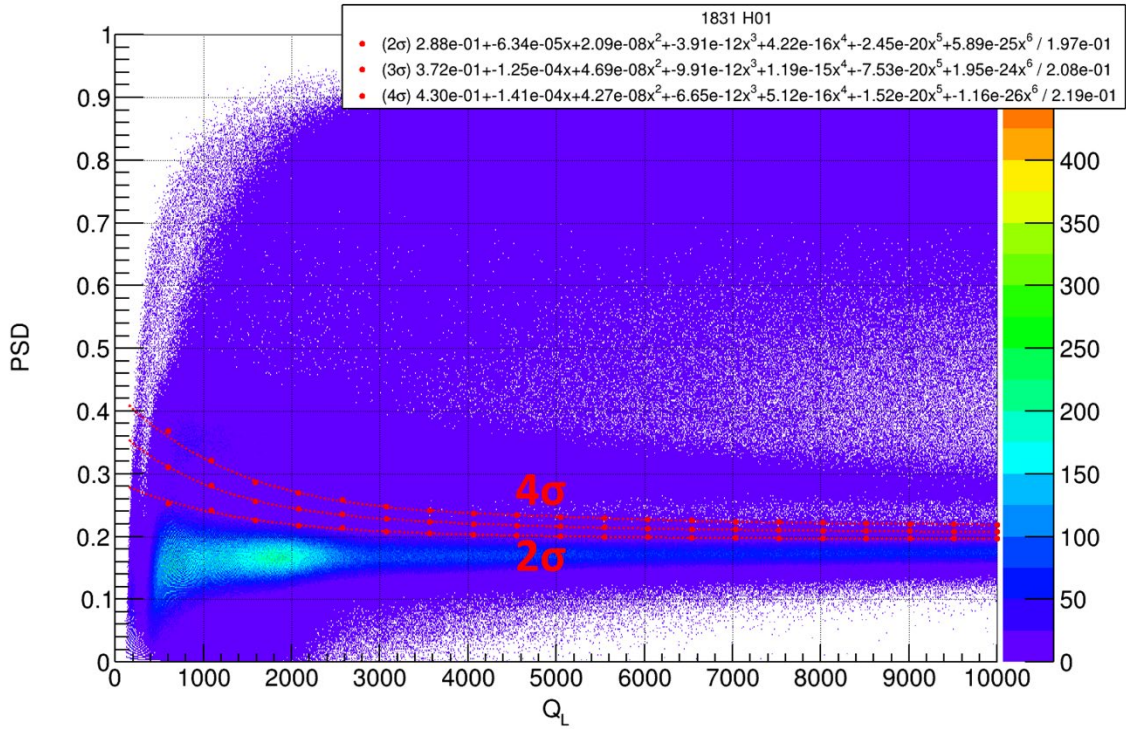


Figure 3. QL vs PSD scattered plot for the 0.60 cm-thick natural uranium sample within the lead box (run 1831). The red curves represent the polynomial fitting for 2, 3 and 4σ levels of confidence of the PSD gaussian fitting.

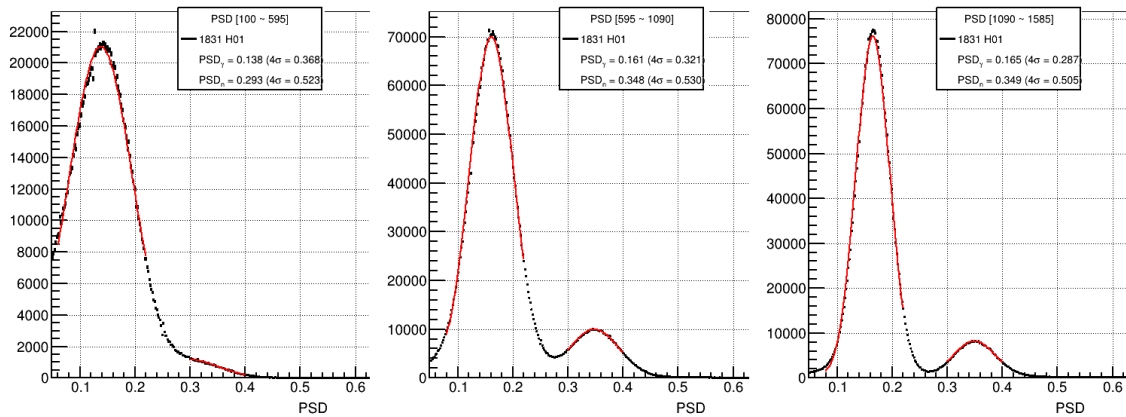


Figure 4. Example of the PSD projection for the first three QL interval gaussian fitting for the neutron and gamma-rays PSD values in the case of 0.60 cm-thick natural uranium sample within the lead box (run 1831). The red curves represent the gaussian fitting results.

Table 2. Selected ²³⁵U neutron resonances from ENDF/B-VIII.0. The values marked with * not used in this linearity study due to poor statistics.

Energy [eV]	Cross Section [barn]	Energy [eV]	Cross Section [barn]
*1.13	1.56x10 ²	7.08	2.28x10 ²
*2.03	9.76x10 ¹	8.76	1.04x10 ³
3.14	8.31x10 ¹	12.39	9.92x10 ²
3.62	1.74x10 ²	19.30	1.24x10 ³
6.39	5.81x10 ²	21.07	5.63x10 ²

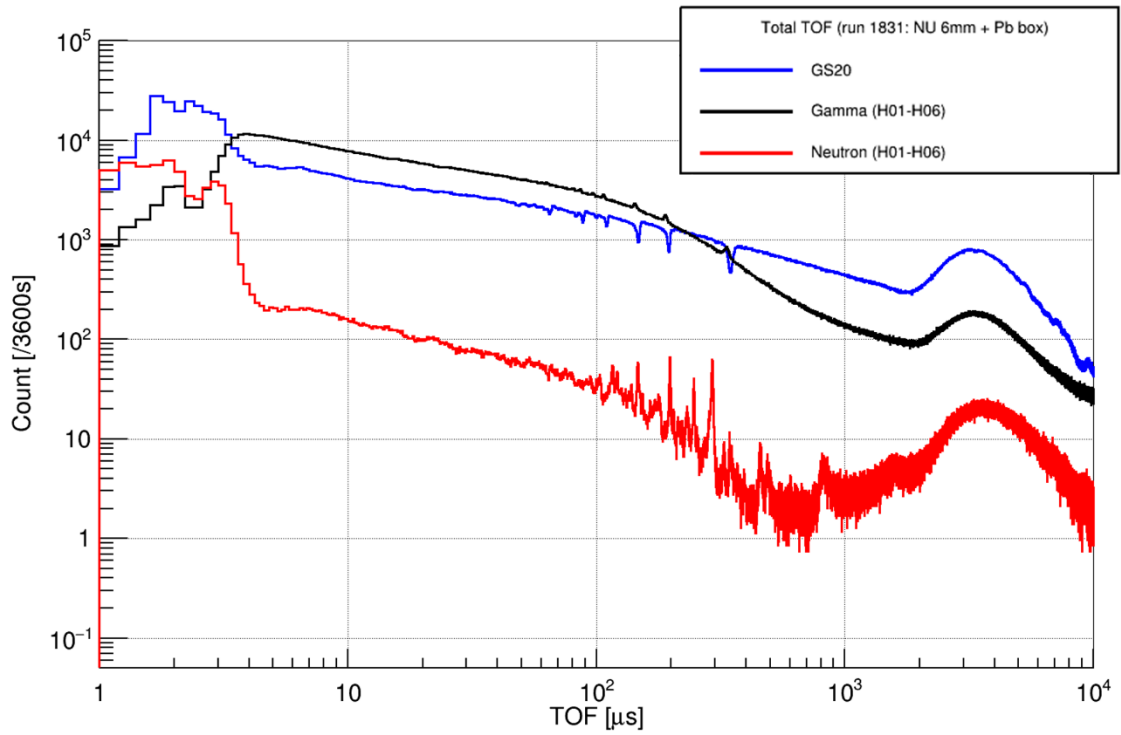


Figure 5. Total TOF spectra for the 0.60 cm-thick natural uranium sample within the lead box. The blue curve represents the transmitted spectrum obtained from the GS20, the black curve and the red curve are the gamma-ray and neutron spectra obtained from the sum of the 6 PSD detectors.

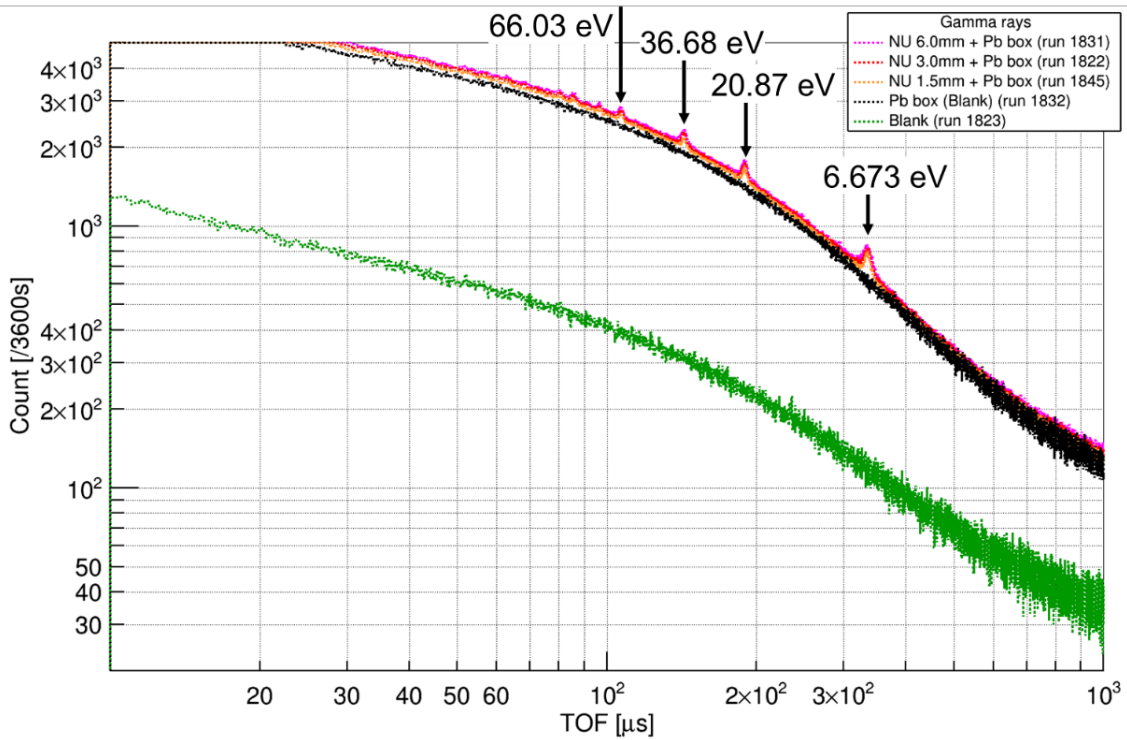


Figure 6. TOF spectra normalized for one-hour measurement time in the gamma-rays gate. The prominent gamma-ray resonances of ^{238}U are labeled.

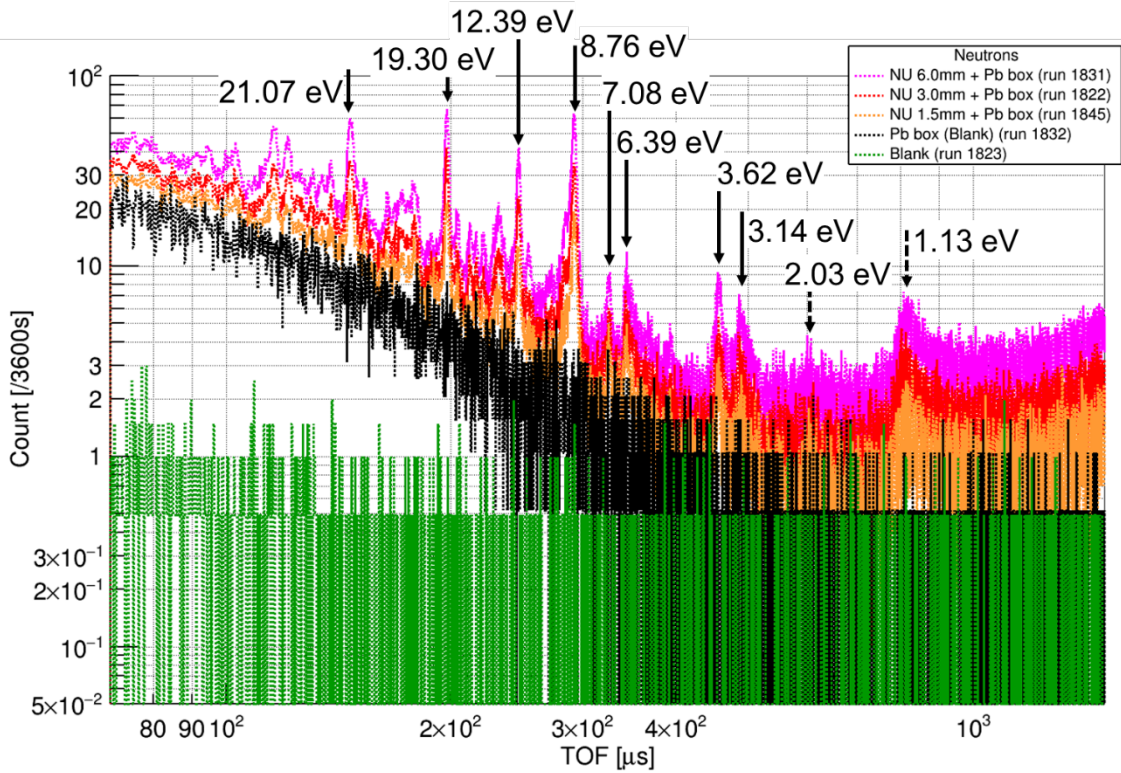


Figure 7. TOF spectra normalized for one-hour measurement time in the neutrons gate. The prominent neutron resonances of ^{235}U are labeled.

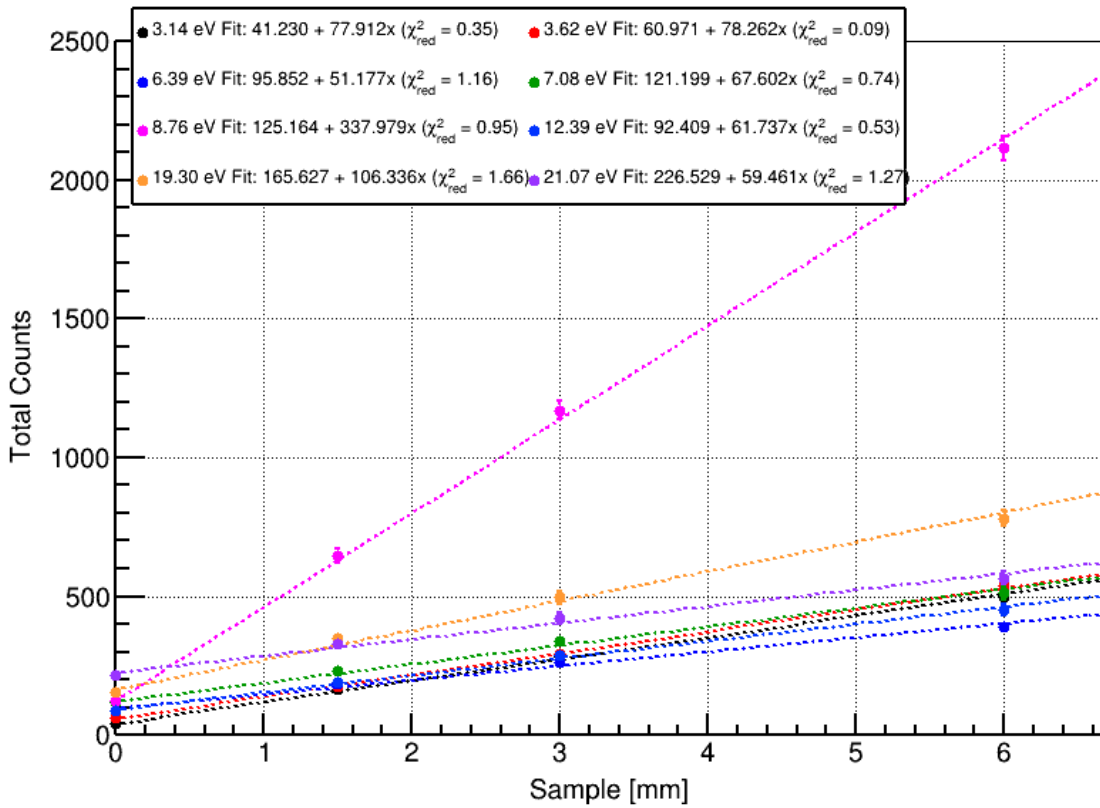


Figure 8. Integrated neutron counts correlation with the sample thickness (mass) for the different ^{235}U neutron resonance energies. The zero thickness is obtained with the irradiation of the only lead box.

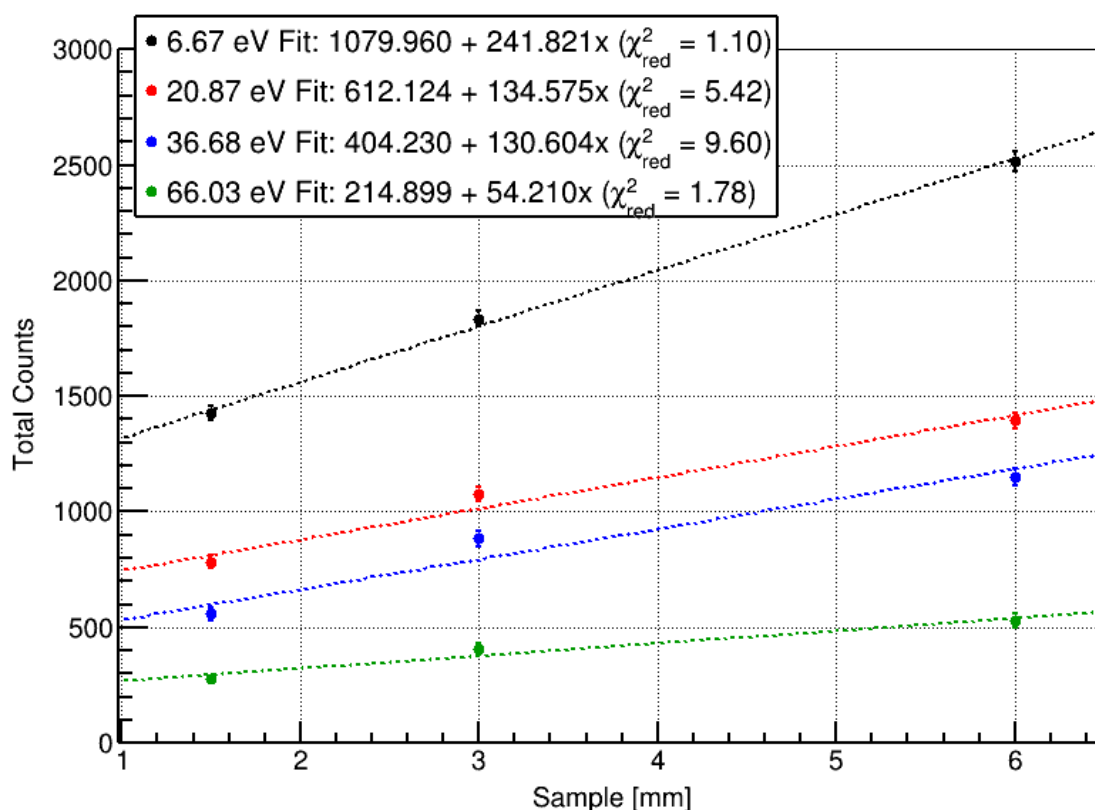


Figure 9. Integrated gamma-ray counts correlation with the sample thickness for the different ^{238}U resonance energies.

5. Conclusion and future work

In this study, we implemented an advanced data-driven pulse shape discrimination (PSD) method, enhancing the analysis of neutron and gamma signals for improved material verification. Our results demonstrate that neutron-based mass correlation (NRFNA) exhibits good linearity and low background, confirming its robustness for fissile material identification, and possibly quantification, in shielded environments. Conversely, gamma-based mass correlation (NRCA) shows a quadratic behavior with high background, indicating the need for further corrections to improve its accuracy. This work also expands the applicability of NRFNA for the verification of shielded nuclear materials, reinforcing its potential role in safeguards and security.

For future research, additional sample masses will be tested to better evaluate the NRCA signal and refine correction methods. Furthermore, low-Z shielding materials will be investigated to assess their impact on measurement performance. Ultimately, we aim to develop a fully integrated detector system combining NRFNA, NRCA, and NRTA, enabling comprehensive material characterization and enhancing the system's effectiveness for nuclear verification applications.

Acknowledgments

The authors would like to thank the LINAC staff of the Institute for Integrated Radiation and Nuclear Science, Kyoto University, for their support in the continuous operation of the accelerator.

This work is supported by the Japanese Ministry of Education, Culture, Sports, Science, and Technology (MEXT) under the subsidy for the "promotion for strengthening nuclear security and the like".

References

- [1] J. W. Sterbentz and D. L. Chichester, "A Second Look at Neutron Resonance Transmission Analysis as a Spent Fuel NDA Technique," in INMM 52nd Annual Meeting, Palm Desert, CA, 2011.
- [2] P. Schillebeeckx, B. Becker, H. Harada and S. Kopecky, "Neutron Resonance Spectroscopy for the Characterisation of Materials and Objects," JRC Science and Policy Reports, JRC 91818, EUR 26848 EN, 2012.
- [3] H. Postma and P. Schillebeeckx, Neutron resonance capture and transmission analysis, New York: John Wiley & Sons Ltd., 2009.
- [4] E. A. Klein, "Neutron Resonance Transmission Analysis of Nuclear Material Using a Portable D-

- T Neutron Generator," Massachusetts Institute of Technology, 2023.
- [5] S. Subzwari, J. Rahon, E. Klein, B. McDonald, M. Zalavadia, M. Moore, J. Kulisek2 and A. Danagoulian, "Neutron Resonance Transmission Analysis for the Thorium Fuel Cycle & High-Gamma Emitting Targets," in INMM Joint Annual Meeting, Portland, 2024.
- [6] H. Postma, M. Blaauw, P. Bode, P. Mutti, F. Corvi and P. Siegler, "Neutron-resonance capture analysis of materials," *Journal of Radioanalytical and Nuclear Chemistry*, vol. 248, no. 1, pp. 115-120, 2001.
- [7] K. Hironaka, J. Lee, M. Koizumi, F. Ito, J. Hori, K. Terada and T. Sano, "Neutron resonance fission neutron analysis for nondestructive fissile material assay," *Nuclear Instruments and Methods in Physics Research Section A: Accelerators, Spectrometers, Detectors and Associated Equipment*, vol. 1054, 2023.
- [8] F. Rossi, J. Lee, Y. Kodama, K. Hironaka, M. Koizumi, J. Hori, K. Terada and S. T., "Development of a Combined Neutron Resonance Analysis Technique as a Non-Destructive Assay for Fissile Material Quantification," in INMM Joint Annual Meeting, Portland, 2024.
- [9] Kyoto University, "Overview of KURNS-LINAC," [Online]. Available: <https://www.rri.kyoto-u.ac.jp/LINAC/spec.html> (in Japanese). [Accessed January 2025].
- [10] T. Sano, J. Hori, Y. Takahashi, H. Yashima, J. Lee and H. Harada, "Analysis of energy resolution in the KURRI-LINAC pulsed neutron facility," *EPJ Web of Conferences*, vol. 146, 2017.
- [11] J. Lee, F. Rossi, Y. Kodama, K. Hironaka, M. Koizumi, T. Sano, Y. Matsuo and J. Hori, "Neutron transmission measurements for silica glass at the KURNS-LINAC," *Annals of Nuclear Energy*, vol. 211, 2025.
- [12] ELJEN Technology, "Pulse Shape Discrimination EJ-276D & EJ-276G," ELJEN, [Online]. Available: <https://eljentechnology.com/products/plastic-scintillators/ej-276>. [Accessed January 2025].
- [13] Hamamatsu Photonics K.K., "Photomultiplier tube assembly H6527," Hamamatsu, [Online]. Available: <https://www.hamamatsu.com/jp/en/product/optical-sensors/pmt/pmt-assembly/head-on-type/H6527.html>. [Accessed January 2025].
- [14] CAEN SpA, "V1730 / V1730S," CAEN SpA, [Online]. Available: <https://www.caen.it/products/v1730/>. [Accessed January 2025].
- [15] R. Brun and F. Rademakers, "ROOT - An Object Oriented Data Analysis Framework," in *AIHENP'96 Workshop*, Lausanne, 1996.
- [16] R. Brun and F. Rademakers, "ROOT — An object oriented data analysis framework," *Nuclear Instruments and Methods in Physics Research Section A: Accelerators, Spectrometers, Detectors and Associated Equipment*, vol. 389, no. 1-2, pp. 81-86, 1997.
- [17] CAEN SpA, CoMPASS Multiparametric DAQ Software for Physics Applications, Rev. 23- April 08th, 2024.
- [18] F. Rossi, J. Lee, Y. Yoshimi, H. K., M. Koizumi, T. Shiba, K. Terada and J. Hori, "Pulse shape discrimination of plastic and glass scintillator for neutron resonance analysis," in *IEEE TRANSACTIONS ON NUCLEAR SCIENCE*, Yokohama, 2025.
- [19] M. S. Moore, "Rate dependence of counting losses in neutron time-of-flight measurements," *Nuclear Instruments and Methods*, vol. 169, pp. 245-247, 1980.
- [20] L. Mihailescu, A. Borella, C. Massimi and P. Schillebeeckx, "Investigations for the use of the fast digitizers with C6D6 detectors for radiative capture measurements at GELINA," *Nuclear Instruments and Methods in Physics Research A*, vol. 600, pp. 453-459, 2009.
- [21] F. Rossi, T. Bogucarska, M. Koizumi, H.-J. Lee, B. Pedersen, D. Rodriguez, T. Takahashi and G. Varasano, "Correlating the fissile mass of standard uranium samples with delayed gamma rays from fission products," *Nuclear Instruments and Methods in Physics Research A*, 2020, DOI: 10.1016/j.nima.2020.164306.